

# PDFs, TMDs, and fragmentation functions of spin-1 hadrons

S. Kumano<sup>1,2</sup>

<sup>1</sup> Department of Mathematics, Physics, and Computer Science, Faculty of Science, Japan Women's University, Mejirodai 2-8-1, Tokyo, 112-8681, Japan

<sup>2</sup>Theory Center, Institute of Particle and Nuclear Studies, High Energy Accelerator Research Organization (KEK), Oho 1-1, Tsukuba, Ibaraki, 305-0801, Japan

June 3, 2024

**Abstract** Structure functions of the spin-1 deuteron will be investigated experimentally from the late 2020's at various facilities such as Thomas Jefferson National Accelerator Facility, Fermi National Accelerator Laboratory, nuclotron-based ion collider facility, and electron-ion colliders. We expect that a new high-energy spin-physics field could be created by these projects. In this paper, the current theoretical status is explained for the structure functions of spin-1 hadrons, especially on parton distribution functions, transverse-momentum dependent parton distributions, and fragmentation functions. Related multiparton distribution functions are also shown.

## 1 Introduction

Structure functions of the spin-1/2 nucleons have been investigated for a long time including the polarized ones. The origin of the nucleon spin has not been identified yet because the gluon-spin and partonic orbital-angular-momentum contributions are not determined yet. It should be clarified by the project of the electron-ion colliders (EICs) [1, 2] in 2030's. In contrast, studies on structure functions of spin-1 hadrons are at a premature stage. It is because there is no experimental measurement on polarized structure functions of spin-1 hadrons since the HERMES  $b_1$  experiment in 2005 [3]. We expect that the situation will change significantly in a few years because of various experimental projects on spin-1 structure functions, such as at the Thomas Jefferson National Accelerator Facility (JLab) [4, 5], the Fermi National Accelerator Laboratory (Fermilab) [6, 7], the nuclotron-based ion collider facility (NICA) [8], and the EICs. It is likely that a new field of high-energy spin physics will be created for spin-1 hadrons such as the deuteron.

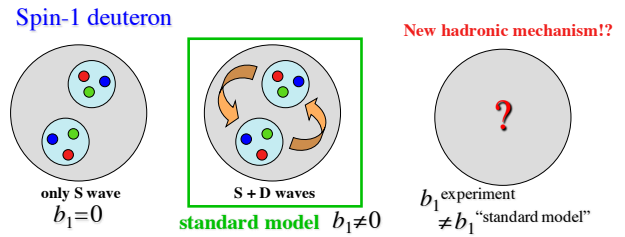


**Fig. 1** New hadron physics by structure function  $b_1$ .

The tensor-polarized leading-twist structure function  $b_1$  does not exist in the spin-1/2 nucleons and it is unique in a spin-1 project [9, 10]. If the spin-1 deuteron is an S-wave bound state of a proton and a neutron,  $b_1$  should vanish ( $b_1 = 0$ ). Since there is a standard deuteron model with the D-state admixture, we can calculate  $b_1$  theoretically by the convolution model. However, such a “standard-model” calculation [11] indicated that the theoretical  $b_1$  distribution could be very different from the HERMES measurement [3]. It possibly suggests that a new hadronic mechanism would be needed for explaining  $b_1$  as illustrated in Fig. 1.

Another interesting observable is the gluon transversity  $\Delta_T g$  [12], which does not exist in the spin-1/2 nucleons, because the change of two spin units is necessary for the helicity flip amplitude as shown in Fig. 2. Since there is no contribution from a proton and a neutron in the deuteron, if a finite  $\Delta_T g$  is found in experiments [1, 2, 5, 7, 8], it means a new hadronic physics beyond the simple bound system of the nucleons. By the measurements of unique spin-1 observables, such as  $b_1$  and  $\Delta_T g$ , we expect that a new hadron-physics field could be created.

In order to prepare for the future experimental projects on spin-1 hadrons, the theoretical status is explained for possible parton distribution functions (PDFs), transverse-momentum-dependent parton distributions (TMDs), and

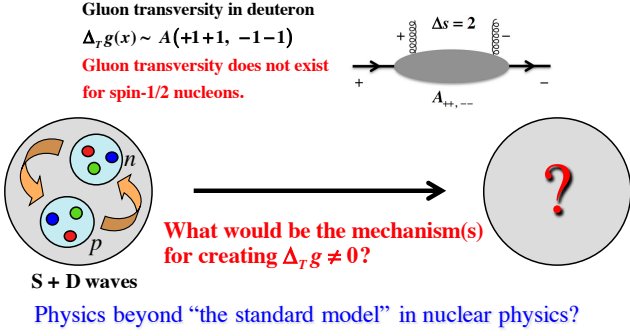


**Fig. 2** New hadron physics by gluon transversity  $\Delta_T g$ .

fragmentation functions (FFs) of spin-1 hadrons in this paper. Related multiparton distribution functions are also shown. This article consists of the following. In Sec. 2, the structure functions  $b_{1-4}(x)$  and the tensor-polarized PDFs are explained. The TMDs for spin-1 hadrons are discussed up to twist 4 in Sec. 3, possible fragmentation functions are shown also up to twist 4 in Sec. 4, and the summary is given in Sec. 5.

## 2 Structure functions for spin-1 hadrons

Deep inelastic charged-lepton scattering from a spin-1 hadron is described by the variables  $x$  and  $Q^2$ , where  $Q^2$  is given by the momentum transfer  $q$  as  $Q^2 = -q^2$  and the Bjorken scaling variable  $x$  is by  $x = Q^2/2M_N q^0$  with the nucleon mass  $M_N$  and the energy transfer  $q^0$ . On the other hand, the scaling variable could be defined as  $x_D = Q^2/(2p \cdot q)$  with the hadron momentum  $p$ . In the deuteron's structure functions, for example, the kinematical range of  $x$  is given by  $0 \leq x \leq 2$  instead of  $0 \leq x_D \leq 1$  because  $x$  is defined by the nucleon mass. It is sometimes confusing in handling nuclear structure functions. The hadron tensor for the charged-lepton deep inelastic scattering for a spin-1 hadron is expressed in terms of eight structure functions,  $F_{1,2}$ ,  $g_{1,2}$ , and  $b_{1-4}$  as [9, 10, 13, 14]

$$\begin{aligned}
 W_{\mu\nu}^{\lambda_f \lambda_i} = & -F_1 \hat{g}_{\mu\nu} + \frac{F_2}{M\nu} \hat{p}_\mu \hat{p}_\nu + \frac{ig_1}{\nu} \epsilon_{\mu\nu\lambda\sigma} q^\lambda s^\sigma \\
 & + \frac{ig_2}{M\nu^2} \epsilon_{\mu\nu\lambda\sigma} q^\lambda (p \cdot q s^\sigma - s \cdot q p^\sigma) \\
 & - b_1 r_{\mu\nu} + \frac{1}{6} b_2 (s_{\mu\nu} + t_{\mu\nu} + u_{\mu\nu}) \\
 & + \frac{1}{2} b_3 (s_{\mu\nu} - u_{\mu\nu}) + \frac{1}{2} b_4 (s_{\mu\nu} - t_{\mu\nu}), \quad (1)
 \end{aligned}$$

where  $r_{\mu\nu}$ ,  $s_{\mu\nu}$ ,  $t_{\mu\nu}$ , and  $u_{\mu\nu}$  are given by

$$\begin{aligned}
 r_{\mu\nu} &= \frac{1}{\nu^2} \left[ q \cdot E^*(\lambda_f) q \cdot E(\lambda_i) - \frac{1}{3} \nu^2 \kappa \right] \hat{g}_{\mu\nu}, \\
 s_{\mu\nu} &= \frac{2}{\nu^2} \left[ q \cdot E^*(\lambda_f) q \cdot E(\lambda_i) - \frac{1}{3} \nu^2 \kappa \right] \frac{\hat{p}_\mu \hat{p}_\nu}{M\nu}, \\
 t_{\mu\nu} &= \frac{1}{2\nu^2} \left[ q \cdot E^*(\lambda_f) \left\{ \hat{p}_\mu \hat{E}_\nu(\lambda_i) + \hat{p}_\nu \hat{E}_\mu(\lambda_i) \right\} \right.
 \end{aligned}$$

$$\begin{aligned}
 & \left. + \left\{ \hat{p}_\mu \hat{E}_\nu^*(\lambda_f) + \hat{p}_\nu \hat{E}_\mu^*(\lambda_f) \right\} q \cdot E(\lambda_i) - \frac{4\nu}{3M} \hat{p}_\mu \hat{p}_\nu \right], \\
 u_{\mu\nu} &= \frac{M}{\nu} \left[ \hat{E}_\mu^*(\lambda_f) \hat{E}_\nu(\lambda_i) + \hat{E}_\nu^*(\lambda_f) \hat{E}_\mu(\lambda_i) \right. \\
 & \left. + \frac{2}{3} \hat{g}_{\mu\nu} - \frac{2}{3M^2} \hat{p}_\mu \hat{p}_\nu \right]. \quad (2)
 \end{aligned}$$

Here,  $\hat{g}_{\mu\nu}$  and  $\hat{a}_\mu$  are defined by  $\hat{g}_{\mu\nu} \equiv g_{\mu\nu} - q_\mu q_\nu / q^2$  and  $\hat{a}_\mu \equiv a_\mu - (a \cdot q / q^2) q_\mu$  so as to ensure the current conservation  $q^\mu W_{\mu\nu} = q^\nu W_{\mu\nu} = 0$ ,  $\epsilon_{\mu\nu\lambda\sigma}$  is an anti-symmetric tensor with the convention  $\epsilon_{0123} = +1$ ,  $\nu$  is defined by  $\nu = p \cdot q / M$  with the spin-1 hadron mass  $M$ ,  $\kappa$  is defined by  $\kappa = 1 + Q^2 / \nu^2$ , and  $s^\mu$  is the spin vector of the spin-one hadron. The initial and final spin states are denoted as  $\lambda_i$  and  $\lambda_f$ , respectively, and off-diagonal terms with  $\lambda_f \neq \lambda_i$  are needed for higher-twist terms [15]. The  $E^\mu$  is the polarization vector of the spin-one hadron

$$E^\mu(\lambda = \pm 1) = \frac{1}{\sqrt{2}}(0, \mp 1, -i, 0), \quad E^\mu(\lambda = 0) = (0, 0, 0, 1), \quad (3)$$

and it satisfies the conditions,  $p \cdot E = 0$  and  $E^* \cdot E = -1$ . The spin vector  $s$  is given by the polarization vector as

$$(s_{\lambda_f \lambda_i})^\mu = -\frac{i}{M} \epsilon^{\mu\nu\alpha\beta} E_\nu^*(\lambda_f) E_\alpha(\lambda_i) p_\beta. \quad (4)$$

The structure functions  $b_1$  and  $b_2$  are twist-2 functions and they satisfy the Callan-Gross type relation  $2x_D b_1 = b_2$  in the Bjorken-scaling limit. The functions  $b_3$  and  $b_4$  are higher-twist ones. The projection operators for  $F_{1,2}$ ,  $g_{1,2}$ , and  $b_{1-4}$  from the hadron tensor  $W_{\mu\nu}^{\lambda_f \lambda_i}$  are shown in Ref. [13].

In the parton model, the structure function  $b_1$  is written in terms of the tensor-polarized distributions  $\delta_T q(x)$  as [10, 16]

$$\begin{aligned}
 b_1(x, Q^2) &= \frac{1}{2} \sum_i e_i^2 [\delta_T q_i(x, Q^2) + \delta_T \bar{q}_i(x, Q^2)], \\
 \delta_T q_i &\equiv q_i^0 - \frac{q_i^{+1} + q_i^{-1}}{2}, \quad (5)
 \end{aligned}$$

where  $i$  is the quark flavor,  $e_i$  is its charge, and  $q_i^\lambda$  indicates an unpolarized-quark distribution in the hadron with the spin state  $\lambda$ . We may note that  $\delta_T q(x)$  is the unpolarized quark distribution in a tensor-polarized hadron. In this equation, the overall factor 1/2 is introduced in  $b_1$  in the same way with  $F_1$  and  $g_1$  in terms of the corresponding PDFs. There are various conventions for the tensor-polarized distribution  $\delta_T q$ , and it is also denoted as  $\delta q$ ,  $\Delta_T q$ , or  $f_{1LL} [= -(2/3)\delta_T q]$ .

## 2.1 Sum rule for $b_1$

Sum rules based on the parton model can be derived by relating a structure function integrated over  $x$  to an elastic form factor in the infinite momentum frame [17] as shown in Fig. 3, and a useful sum rule was derived for  $b_1$  by using this method [16]. It is not a rigorous sum rule, and it is intended to supply a basic idea on  $b_1$  and tensor-polarized PDFs in the same way with the Gottfried sum rule [18–20].

A rough sum-rule form could be guessed in an intuitive way by the dimensional counting. In the hadron tensor of Eq. (1),  $b_1$  is defined as a dimensionless quantity, so that its first moment also does not have mass dimension. Its sum should be expressed by a global electromagnetic observable to satisfy the parity and time-reversal invariances, namely by the the electric quadrupole moment  $Q_h$  of the hadron  $h$ , for a tensor-polarized spin-1 hadron. The  $Q_h$  has the dimension of length<sup>2</sup> = 1/mass<sup>2</sup>, so that it should be cancelled by a mass<sup>2</sup> factor as  $\int dx b_1(x) = (\text{mass dim.})^2 Q_h$ . From the elastic process in Fig. 3, this mass-dimension squared factor could be either the hadron mass squared  $M^2$  or the momentum transfer squared  $t$ .

By the optical theorem, the hadron tensor is equal to the imaginary part of the forward scattering amplitude for virtual photon scattering. It indicates that the first moment of a structure function is related to an elastic form factor expressed by the PDFs in the infinite-momentum frame as illustrated in Fig. 3. For example, the polarized Bjorken sum rule was derived by this method in Ref. [17]. This method was applied for  $b_1$  of the deuteron [16]. Here, the structure function  $b_1$  and the PDFs are defined by the ones per nucleon and the scaling variable  $x$  is used. As illustrated in the left-hand side of Fig. 3, integrating Eq. (5) over  $x$  and using the relations  $(\delta_T u_v)_D \equiv (\delta_T u - \delta_T \bar{u})_D = (\delta_T u_v^p + \delta_T u_v^n)/2 = (\delta_T u_v + \delta_T d_v)/2$ ,  $(\delta_T d_v)_D = (\delta_T d_v + \delta_T u_v)/2$  for the valence-quark distributions, we obtain

$$\int dx b_1(x) = \frac{5}{36} \int dx [\delta_T u_v(x) + \delta_T d_v(x)] + \sum_i e_i^2 \int dx \delta_T \bar{q}_{i,D}(x), \quad (6)$$

where  $Q^2$  dependence is not explicitly shown and the relation  $\int dx (\delta_T s - \delta_T \bar{s})_D = \int dx (\delta_T c - \delta_T \bar{c})_D = \int dx (\delta_T b$

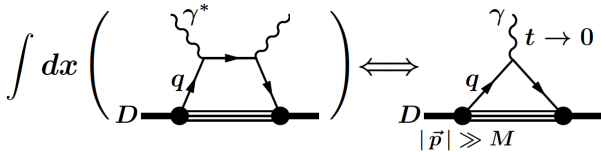


**Fig. 3** Relation between the first moment of a structure function and an elastic form factor.

$-\delta_T \bar{b})_D = 0$  is used. The function  $q_v$  indicates a valence-quark distribution, and the valence-quark distributions in the deuteron come from the corresponding ones in the proton and the neutron.

The helicity amplitude with the charge operator  $J_0$  is defined for the elastic scattering in the right-hand side of Fig. 3. If the frame with a large longitudinal momentum  $|\vec{p}| \gg M$  is taken, the elastic amplitude is calculated by the parton model as [17]

$$\Gamma_{H,H} \equiv \langle p, H | J_0(0) | p, H \rangle = \sum_i e_i \int dx [q_i^H(x) - \bar{q}_i^H(x)]_D. \quad (7)$$

The tensor combination of the amplitudes is expressed in terms of the valence-quark distributions in the deuteron by considering the proton and neutron contributions as  $\Gamma_{0,0} - (\Gamma_{1,1} + \Gamma_{-1,-1})/2 = \frac{1}{3} \int dx [\delta_T u_v(x) + \delta_T d_v(x)]$  with the condition  $\int dx (\delta_T s - \delta_T \bar{s})_D = \int dx (\delta_T c - \delta_T \bar{c})_D = \int dx (\delta_T b - \delta_T \bar{b})_D = 0$ . Substituting this helicity relation into Eq. (6), we obtain  $\int dx b_1(x) = (5/12) [\Gamma_{0,0} - (\Gamma_{1,1} + \Gamma_{-1,-1})/2] + \sum_i e_i^2 \int dx \delta_T \bar{q}_{i,D}(x)$ .

The helicity amplitudes are expressed by the electric charge and quadrupole form factors of the deuteron,  $F_C(t)$  and  $F_Q(t)$  expressed by the momentum-transfer squared  $t$  ( $\rightarrow 0$ ), as

$$\Gamma_{0,0} = \lim_{t \rightarrow 0} \left[ F_C(t) - \frac{t}{3M^2} F_Q(t) \right], \quad \Gamma_{1,1} = \Gamma_{-1,-1} = \lim_{t \rightarrow 0} \left[ F_C(t) + \frac{t}{6M^2} F_Q(t) \right], \quad (8)$$

where  $F_C(t)$  and  $F_Q(t)$  are defined by the units of  $e$  and  $e/M^2$ , respectively, with the elementary charge  $e$  and the deuteron mass  $M$ . The tensor-polarization combination of the helicity amplitudes is given by the quadrupole form factor as  $\Gamma_{0,0} - (\Gamma_{1,1} + \Gamma_{-1,-1})/2 = -\lim_{t \rightarrow 0} \frac{t}{4} F_Q(t) = 0$ . Using this relation, we obtain the sum rule

$$\int dx b_1(x) = -\lim_{t \rightarrow 0} \frac{5}{24} t F_Q(t) + \sum_i e_i^2 \int dx \delta_T \bar{q}_{i,D}(x). \quad (9)$$

If the tensor-polarized antiquark distributions vanish  $\int dx \delta_T \bar{q}_{i,D}(x) = 0$ , the sum becomes

$$\int dx b_1(x) = 0. \quad (10)$$

This  $b_1$  sum rule is similar to the Gottfried sum rule which was also derived by the parton model:

$$\int dx b_1(x) = 0 + \sum_i e_i^2 \int dx \delta_T \bar{q}_{i,D}(x), \quad \int \frac{dx}{x} [F_2^p(x) - F_2^n(x)] = \frac{1}{3} + \frac{2}{3} \int dx [\bar{u}(x) - \bar{d}(x)]. \quad (11)$$

The finite Gottfried sum  $1/3$  is due to the flavor dependence of the valence quark distributions,  $\int [u_v(x) - d_v(x)]/3 = 1/3$ . On the other hand, the  $b_1$  sum vanishes  $-\lim_{t \rightarrow 0} (5/24)tF_Q(t) = 0$  because the valence-quark number does not depend on the tensor polarization. The second moment of  $b_1$  was also shown to vanish  $\int dx x b_1(x) = 0$  [21], which could be related to an interesting shear-force property [8].

We may note that both sum rules are not rigorous ones and they are based on the parton model. The integrals  $\int dx \delta_T \bar{q}_{i,D}(x)$  and  $\int dx [\bar{u}(x) - \bar{d}(x)]$  could diverge depending on the functional form of  $x$  at small  $x$ , especially as  $Q^2$  increases. This was studied in Ref. [22] in a convolution model. Although both sum rules may not be satisfied especially at large  $Q^2$ , we know, nonetheless, that the Gottfried sum rule was very useful for indicating the difference between  $\bar{u}$  and  $\bar{d}$  from its violation in DIS experiments, and such studies created a new field in hadron physics on flavor asymmetric antiquark distributions ( $\bar{u} - \bar{d}$ ) in the nucleon [18–20].

In the same way, the finite sum of  $b_1$  could indicate the tensor-polarized antiquark distributions  $\delta_T \bar{q}_{i,D}(x)$ , and the sum for the valence-quark part ( $\int b_{1,\text{val}} = 0$ ) provides a guideline on the functional form of the tensor-polarized valence-quark distributions as used, for example, in Sec. 2.2. On the antiquark distributions, there was already a hint from the HERMES measurement as [3]  $\int_{0.02}^{0.85} dx b_1(x) = [0.35 \pm 0.10 \text{ (stat)} \pm 0.18 \text{ (sys)}] \times 10^{-2}$  by taking the the range  $Q^2 > 1 \text{ GeV}^2$ . If the JLab experiment finds a finite sum with a reasonable precision [4], the mechanism of creating a finite  $\delta_T \bar{q}_{i,D}(x)$  will become an interesting theoretical topic.

## 2.2 Parametrization for tensor-polarized PDFs

The HERMES data [3] are the only available ones for the structure function  $b_1$ , so that a real global analysis cannot be done for the tensor-polarized PDFs at this stage. However, it is useful to provide appropriate tensor-polarized PDFs for planning future experiments and for testing theoretical model and possible lattice-QCD calculations. We take the PDF parametrization form as [23]

$$\begin{aligned} \delta_T q_{iv}^D(x) &= \delta_T w(x) q_{iv}^D(x), \\ \delta_T \bar{q}_i^D(x) &= \alpha_{\bar{q}} \delta_T w(x) \bar{q}_i^D(x), \end{aligned} \quad (12)$$

at the initial scale  $Q_0^2$  by considering that certain fractions of the unpolarized PDFs are tensor polarized. At this stage, there is no data to indicate the tensor-polarized gluon distribution  $\delta_T g$ , so that  $\delta_T g = 0$  is assumed at  $Q_0^2$ . It means that a finite  $\delta_T g$  exists at a different scale  $Q^2$  as shown in Ref. [24]. We assumed the common function  $\delta_T w(x)$  for both the valence-quark and antiquark

distributions. The  $\alpha_{\bar{q}}$  is a parameter for the difference between the overall valence-quark and antiquark distributions, and its flavor dependence was not considered. Neglecting small nuclear corrections, of the order of a few percent in the deuteron, we write the PDFs of the deuteron as  $q_i^D = (q_i^p + q_i^n)/2$  and  $\bar{q}_i^D = (\bar{q}_i^p + \bar{q}_i^n)/2$ . Then, the isospin symmetry is used for the PDFs in the neutron and flavor symmetric tensor-polarized distributions are taken as

$$\begin{aligned} \delta_T q_v^D(x) &\equiv \delta_T u_v^D(x) = \delta_T d_v^D(x) = \delta_T w(x) \frac{u_v(x) + d_v(x)}{2}, \\ \delta_T \bar{q}^D(x) &\equiv \delta_T \bar{u}^D(x) = \delta_T \bar{d}^D(x) = \delta_T s^D(x) = \delta_T \bar{s}^D(x) \\ &= \alpha_{\bar{q}} \delta_T w(x) \frac{2\bar{u}(x) + 2\bar{d}(x) + s(x) + \bar{s}(x)}{6}. \end{aligned} \quad (13)$$

The tensor-polarized charm and bottom quark distributions are neglected.

The leading-order (LO) expression for  $b_1$  of Eq. (5) is given by these PDFs as

$$\begin{aligned} b_1^D(x) &= \frac{1}{36} \delta_T w(x) [5\{u_v(x) + d_v(x)\} \\ &\quad + 4\alpha_{\bar{q}}\{2\bar{u}(x) + 2\bar{d}(x) + s(x) + \bar{s}(x)\}]. \end{aligned} \quad (14)$$

Because there is no experimental indication for the scaling violation, the  $Q^2$  dependence is ignored. The scale  $Q_0^2$  is taken as the average one  $Q_0^2 = 2.5 \text{ GeV}^2$  of the HERMES experimental values. As shown in Sec. 2.1, the tensor-polarized valence-quark distributions satisfy the relation  $\int dx (b_1)_{\text{valence}} = 0$ , so that the weight function  $\delta_T w(x)$  could be parametrized as

$$\delta_T w(x) = ax^b(1-x)^c(x_0-x), \quad (15)$$

with the parameters  $a$ ,  $b$ , and  $c$ , which are determined by a  $\chi^2$  analysis. The node factor  $x_0$  is expressed in terms of these parameters by the condition  $\int dx (b_1)_{\text{valence}} = 0$ . For satisfying this integral, a node should exist in the tensor-polarized PDFs and it is also supported by the convolution model [11].

The parameters were determined by analyzing the HERMES data with ( $\alpha_{\bar{q}} \neq 0$ ) or without ( $\alpha_{\bar{q}} = 0$ ) the tensor-polarized antiquark distributions in Ref. [23] and the optimum one was with  $\alpha_{\bar{q}} \neq 0$  (set 2). The parametrized  $b_1$  is calculated with the determined parameters and it is compared with the HERMES data in Fig. 4 [23, 24]. The obtained tensor-polarized PDFs are shown in Fig. 5 with their uncertainties. The solid and dotted curves are the tensor-polarized valence-quark and antiquark distributions, respectively. Although the errors are still large, the HERMES data seem to indicate the existence of finite tensor-polarized antiquark distributions. From the parametrized  $b_1$ , we obtain the sum  $\int dx b_1(x) = 0.0058$ , which suggests the finite tensor-polarized antiquark distributions according to Eq. (11).

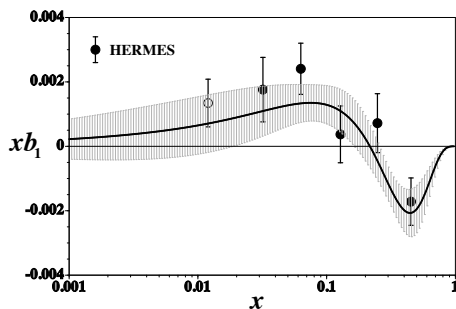


**Fig. 4** HERMES data and parametrized  $b_1$  structure function with its uncertainty band. The data with  $Q^2 < 1 \text{ GeV}^2$  is shown by the open circle.

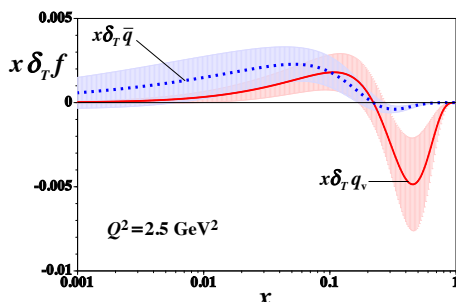


**Fig. 5** Determined tensor polarized distributions are shown with their uncertainties.

The JLab experiment will measure  $b_1$  in the range  $0.1 < x < 0.5$  more accurately [4], so that we expect to obtain reliable tensor-polarized PDFs in the near future. Furthermore, there are projects with the polarized deuteron target and beam at Fermilab [6, 7] and NICA [8] for investigating the tensor-polarized PDFs, for example, by the proton-deuteron Drell-Yan process [25, 26].

### 2.3 Theoretical $b_1$ by the standard deuteron model

In order to find a new aspect of hadronic physics by the structure function  $b_1$  in comparison with the HERMES and future data,  $b_1$  was calculated by the standard deuteron model in the convolution formalism [11]. For describing nuclear structure functions, the convolution model is usually used by expressing the nuclear hadronic tensor  $W_{\mu\nu}^A$  as a convolution of a nuclear spectral function  $S(p)$  and the nucleonic hadronic tensor  $W_{\mu\nu}^N$ :

$$W_{\mu\nu}^A(P_A, q) = \int d^4p S(p) W_{\mu\nu}^N(p, q). \quad (16)$$

Two theoretical calculations were provided in Ref. [11].

In the first convolution method (Theory 1), scaling-limit relations between virtual photon-hadron helicity amplitudes and the structure functions of the deuteron/nucleon are used. Then,  $b_1$  is written by the convolution integral of the lightcone momentum distribution of the nucleon  $f^H(y)$ , where  $H$  is the deuteron polarization, with

the average of proton and neutron structure functions  $F_1^N = (F_1^p + F_1^n)/2$  as

$$b_1(x, Q^2) = \int \frac{dy}{y} \left[ f^0(y) - \frac{f^+(y) + f^-(y)}{2} \right] F_1^N(x/y, Q^2). \quad (17)$$

The distribution  $f^H(y)$  is given by the deuteron wave function  $\phi^H(\mathbf{p})$  with the normalization  $\int d^3\mathbf{p} y |\phi^H(\mathbf{p})|^2 = 1$  as

$$f^H(y) = \int d^3\mathbf{p} y |\phi^H(\mathbf{p})|^2 \delta\left(y - \frac{\sqrt{m_N^2 + \mathbf{p}^2} - p_z}{m_N}\right). \quad (18)$$

The LO expression is used for  $F_1^N$  from the PDFs by considering the transverse-longitudinal cross section ratio  $R = \sigma_L/\sigma_T$  as

$$F_1^N(x, Q^2) = \frac{1 + 4m_N^2 x^2/Q^2}{2x[1 + R(x, Q^2)]} \times \sum_i e_i^2 x [q_i(x, Q^2) + \bar{q}_i(x, Q^2)]. \quad (19)$$

In the second convolution method (Theory 2), the virtual nucleon approximation is used. It considers the  $np$  component of the light-front deuteron wave function, and the virtual photon interacts with one nucleon ( $i$ ) which is off the mass shell, while the second noninteracting spectator nucleon ( $N$ ) is assumed to be on its mass shell. In this method, no scaling limit relations are used, so that higher-twist nuclear effects are included. Its  $b_1$  expression is given by

$$b_1(x, Q^2) = \frac{3}{4(1 + Q^2/\nu^2)} \int \frac{k^2}{\alpha_i} dk d(\cos\theta_k) \times \left[ F_1^N(x_i, Q^2) (6 \cos^2\theta_k - 2) + \frac{\mathbf{p}_i^{\perp 2}}{2p_i q} F_2^N(x_i, Q^2) \times (5 \cos^2\theta_k - 1) \right] \left[ \frac{U(k)W(k)}{\sqrt{2}} + \frac{W(k)^2}{4} \right], \quad (20)$$

where  $\nu$  is the virtual photon energy in the deuteron rest frame,  $p_i$  is the four-momentum of the struck nucleon,  $x_i = Q^2/(2p_i \cdot q)$  is the Bjorken variable, and  $\alpha_i = 2p_i^-/P^-$  is the lightcone momentum fraction with  $P = p_i + p_N$ . The momentum  $k$  corresponds to the relative momentum of the two nucleons with identical light-front momentum components ( $P^-, P^\perp$ ). The radial  $S$ - and  $D$ -wave light-front deuteron wave functions are denoted as  $U(k)$  and  $W(k)$ , and they satisfy the baryon and momentum sum rules. The difference between both methods in Eqs. (17) and (20) comes mainly in the  $F_2^N$  term which reflects the higher-twist nuclear effects.

For the numerical evaluations, we used the MSTW-2008 (Martin-Stirling-Thorne-Watt, 2008) LO parametrization for  $F_2^N$ , the SLAC-R1998 parametrization for  $R$ , and the CD-Bonn deuteron wave function. The  $S$  and  $D$

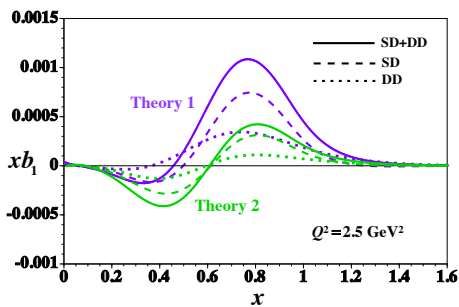


Fig. 6  $S$  and  $D$  wave contributions to  $b_1$ .

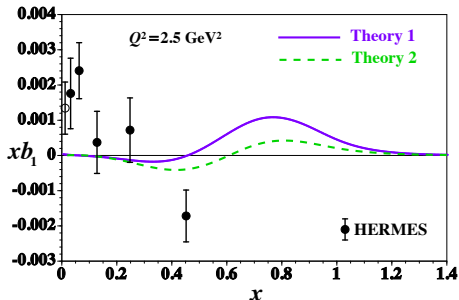


Fig. 7 Standard deuteron model calculations at  $Q^2 = 2.5 \text{ GeV}^2$  are compared with the HERMES data.

wave contributions to  $b_1$  are shown at  $Q^2 = 2.5 \text{ GeV}^2$  in Fig. 6. The  $SD$  interference contribution is large; however, the pure  $D$  wave term is also comparable in magnitude. The total contributions are compared with the HERMES data at  $Q^2 = 2.5 \text{ GeV}^2$  in Fig. 7. The differences between the two theoretical results should come mainly from higher-twist effects. It is interesting to find sizable distributions even at  $x > 1$ . We also notice the theoretical curves are very different from the HERMES measurements. Since our theoretical estimates are based on the standard deuteron model, the deviations from the experimental data may indicate a new hadron mechanism in  $b_1$ , although it would be too early to conclude the existence of such a new mechanism because the errors of the HERMES data are large and careful studies would be necessary for estimating the higher-twist effects in extracting  $b_1$  from experimental measurements. On the other hand, there is an interesting suggestion that  $b_1$  could contain a new hadronic mechanism, such as the hidden color [22].

#### 2.4 Gluon transversity

The quark transversity distributions have been investigated experimentally for the spin-1/2 nucleon; however, there is no experimental measurement for the gluon transversity  $\Delta_T g(x)$ . Because it is given by the gluon-helicity flip amplitude

$$\Delta_T g(x) \sim \text{Im} A_{++,-,-}, \quad (21)$$

the change of two spin units ( $\Delta s = 2$ ) is needed as illustrated in Fig. 2. Here,  $A_{A_i \lambda_i, A_f \lambda_f}$  is the parton-hadron forward scattering amplitude with the initial and final hadron helicities  $A_i$  and  $A_f$  and parton ones  $\lambda_i$  and  $\lambda_f$ . This spin-flip process is not possible in the spin-1/2 nucleon; however, this gluon transversity exists in the spin-1 deuteron. It is a unique project in the deuteron. As explained in the introduction, this situation makes it an interesting observable to find an exotic hadron physics mechanism.

The gluon transversity is defined by the matrix element between the linearly polarized ( $E_x$ ) deuteron as [27]

$$\Delta_T g(x) = \varepsilon_{TT}^{\alpha\beta} \int \frac{d\xi^-}{2\pi} x p^+ e^{i x p^+ \xi^-} \times \langle p E_x | A_\alpha(0) A_\beta(\xi) | p E_x \rangle_{\xi^+ = \bar{\xi}^- = 0}, \quad (22)$$

where  $p$  is the deuteron momentum,  $A^\mu$  is the gluon field,  $x$  is the momentum fraction for a gluon,  $\varepsilon_{TT}^{\alpha\beta}$  is the transverse parameter with  $\varepsilon_{TT}^{11} = +1$  and  $\varepsilon_{TT}^{22} = -1$ , and  $\xi$  is the space-time coordinate expressed by the lightcone coordinates  $\xi^\pm = (\xi^0 \pm \xi^3)/\sqrt{2}$  and  $\vec{\xi}_\perp$ . It is written by the gluon distribution difference as

$$\Delta_T g(x) = g_{\hat{x}/\hat{x}}(x) - g_{\hat{y}/\hat{x}}(x), \quad (23)$$

with the notation  $\hat{y}/\hat{x}$  which indicates the gluon linear polarization  $\varepsilon_y$  in the deuteron with the deuteron polarization  $E_x$ . Therefore, it is actually the gluon linearity but it is usually called the gluon transversity. We may note that there are various notations for the same gluon transversity as  $\Delta_2 G(x)$  [28, 29],  $a(x)$  [12, 30],  $\Delta_L g(x)$  [31],  $-\delta G(x)$  [32, 33],  $-h_{1TT,g}(x)$  [34–36], and  $\Delta_T g(x)$  [27, 37] used in this paper.

In order to understand the linear polarization in comparison with the longitudinal and transverse polarizations, we list them in terms of the polarization vectors and the spin-vector/tensor parameters of a spin-1 hadron in Table 1. The polarization parameters ( $S_T^x$ ,  $S_T^y$ ,  $\dots$ ) are given in the spin vector  $\mathbf{S}$  and tensor  $T_{ij}$  defined by the polarization vector  $\mathbf{E}$  as [34]

$$\begin{aligned} \mathbf{S} &= \text{Im} (\mathbf{E}^* \times \mathbf{E}) = (S_T^x, S_T^y, S_L), \\ T_{ij} &= \frac{1}{3} \delta_{ij} - \text{Re} (E_i^* E_j) \\ &= \frac{1}{2} \begin{pmatrix} -\frac{2}{3} S_{LL} + S_{TT}^{xx} & S_{TT}^{xy} & S_{LT}^x \\ S_{TT}^{xy} & -\frac{2}{3} S_{LL} - S_{TT}^{xx} & S_{LT}^y \\ S_{LT}^x & S_{LT}^y & \frac{4}{3} S_{LL} \end{pmatrix}. \end{aligned} \quad (24)$$

The linear polarizations are expressed by  $\mathbf{E}_x = (1, 0, 0)$  and  $\mathbf{E}_y = (0, 1, 0)$ , and they contain the linear polarization parameter  $S_{TT}^{xx}$ . However, they also have the tensor polarization parameter  $S_{LL}$ , so that the cross section combination  $d\sigma(E_x) - d\sigma(E_y)$  needs to be taken

Polarizations	$\mathbf{E}$	$S_T^x$	$S_T^y$	$S_L$	$S_{LL}$	$S_{TT}^{xx}$
Longitudinal $+z$	$\frac{1}{\sqrt{2}}(-1, -i, 0)$	0	0	+1	$+\frac{1}{2}$	0
Longitudinal $-z$	$\frac{1}{\sqrt{2}}(+1, -i, 0)$	0	0	-1	$+\frac{1}{2}$	0
Transverse $+x$	$\frac{1}{\sqrt{2}}(0, -1, -i)$	+1	0	0	$-\frac{1}{4}$	$+\frac{1}{2}$
Transverse $-x$	$\frac{1}{\sqrt{2}}(0, +1, -i)$	-1	0	0	$-\frac{1}{4}$	$+\frac{1}{2}$
Transverse $+y$	$\frac{1}{\sqrt{2}}(-i, 0, -1)$	0	+1	0	$-\frac{1}{4}$	$-\frac{1}{2}$
Transverse $-y$	$\frac{1}{\sqrt{2}}(-i, 0, +1)$	0	-1	0	$-\frac{1}{4}$	$-\frac{1}{2}$
Linear $x$	(1, 0, 0)	0	0	0	$+\frac{1}{2}$	-1
Linear $y$	(0, 1, 0)	0	0	0	$+\frac{1}{2}$	+1

**Table 1** Longitudinal, transverse, and linear polarizations of a spin-1 hadron in terms of the polarization vectors  $\mathbf{E}$  and the spin-vector/tensor parameters ( $S_T^x, S_T^y, \dots$ ) [27].

for extracting the pure linear polarization component. We also notice that the transverse polarizations contain the linear polarization parameter  $S_{TT}^{xx}$  in addition to the vector polarization parameters  $S_T^i$  and the tensor polarization parameter  $S_{LL}$ .

There is a project to measure the gluon transversity at JLab in the electron-deuteron scattering by observing the dependence on the angle [5, 38], which is between the lepton-scattering plane and the target-spin orientation. On the other hand, it is possible to investigate the gluon transversity at Fermilab in the Spin-Quest project [7]. The cross section for the proton-deuteron Drell-Yan process  $p(A) + d(B) \rightarrow \mu^+ \mu^- + X$  is given by the linear-polarization difference  $d\sigma(E_x) - d\sigma(E_y)$  and the gluon transversity  $\Delta_T g$  as [27]

$$\frac{d\sigma_{pd \rightarrow \mu^+ \mu^- X}}{d\tau d\mathbf{q}_T^2 d\phi dy} (E_x - E_y) = -\frac{\alpha^2 \alpha_s C_F q_T^2}{6\pi s^3} \cos(2\phi) \times \int_{\min(x_a)}^1 dx_a \frac{\sum_q e_q^2 x_a [q_A(x_a) + \bar{q}_A(x_a)] x_b \Delta_T g_B(x_b)}{(x_a x_b)^2 (x_a - x_1)(\tau - x_a x_2)}. \quad (25)$$

The variable  $\tau$  is given the dimuon mass and the center-of-mass energy squared as  $\tau = M_{\mu\mu}^2/s = Q^2/s$ ,  $\mathbf{q}_T^2$  is the dimuon transverse momentum squared,  $\phi$  is its azimuthal angle,  $y$  is the rapidity in the center-of-mass frame, and the color factor is  $C_F = (N_c^2 - 1)/(2N_c)$  with  $N_c = 3$ . The quark and antiquark distribution functions in the proton,  $q_A(x_a)$  and  $\bar{q}_A(x_a)$ , are well known, so that the gluon transversity in the deuteron  $\Delta_T g(x_b)$  could be found from the cross-section measurement.

The cross sections are calculated by using the CTEQ14 PDFs for the unpolarized PDFs of the proton, and the gluon transversity in the deuteron is assumed as the longitudinally-polarized gluon distribution given by the NNPDF1.1 because there is no available  $\Delta_T g(x_b)$ . It is possibly an overestimation of the cross section. The polarization asymmetry  $A_{E_{xy}} \equiv d\sigma(E_x - E_y)/d\sigma(E_x + E_y)$  is shown for  $p_p = 120$  GeV,  $\phi = 0$ ,  $y = 0.5$ , and

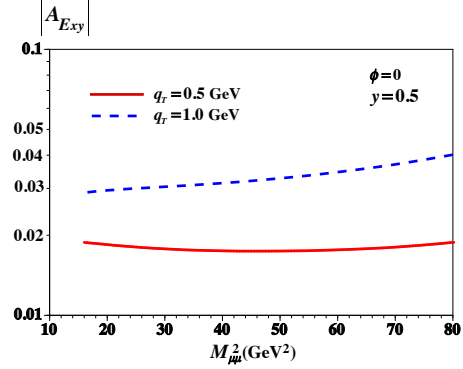


**Fig. 8** Polarization asymmetry  $|A_{E_{xy}}|$  in the proton-deuteron Drell-Yan cross section.

$q_T = 0.5$  or  $1.0$  GeV as the function  $M_{\mu\mu}^2$  in Fig. 8 by considering the Fermilab experiment. The asymmetry is of the order of a few percent. This kind of experiment is also possible at NICA [8]. Possibly, the JLab, Fermilab, NICA, and EIC experiments could create a new field of hadron physics if a finite gluon transversity is found.

### 3 TMDs and PDFs up to twist 4

#### 3.1 Classifications of TMDs and PDFs

Possible TMDs and PDFs up to twist 4 were listed in Ref. [39] for spin-1 hadrons. They were derived in general from a correlation function defined by the amplitude to extract a parton from a hadron and then to insert it into the hadron at a different space-time point as

$$\Phi_{ij}^{[c]}(k, P, T | n) = \int \frac{d^4\xi}{(2\pi)^4} e^{ik \cdot \xi} \times \langle P, T | \bar{\psi}_j(0) W^{[c]}(0, \xi) \psi_i(\xi) | P, T \rangle, \quad (26)$$

where  $P$  and  $T$  indicate the spin-1 hadron momentum and tensor polarization. The vector polarization is not explicitly written. The  $k$  and  $\psi$  are quark momentum and field, and  $W^{[c]}(0, \xi)$  is the gauge link with the integral path  $c$ . The covariant form of the tensor polarization of Eq. (24) is written as

$$T^{\mu\nu} = \frac{1}{2} \left[ \frac{4}{3} S_{LL} \frac{(P^+)^2}{M^2} \bar{n}^\mu \bar{n}^\nu - \frac{2}{3} S_{LL} (\bar{n}^{\{\mu} n^{\nu\}} - g_T^{\mu\nu}) + \frac{1}{3} S_{LL} \frac{M^2}{(P^+)^2} n^\mu n^\nu + \frac{P^+}{M} \bar{n}^{\{\mu} S_{LT}^{\nu\}} - \frac{M}{2P^+} n^{\{\mu} S_{LT}^{\nu\}} + S_{TT}^{\mu\nu} \right], \quad (27)$$

where  $n$  and  $\bar{n}$  are the lightcone vectors  $n^\mu = (1, 0, 0, -1)/\sqrt{2}$  and  $\bar{n}^\mu = (1, 0, 0, 1)/\sqrt{2}$ ,  $g_T^{\mu\nu}$  is given by  $g_T^{11} = g_T^{22} = -1$  and the others = 0,  $a^{\{\mu b^{\nu\}}$  indicates  $a^{\{\mu b^{\nu\}} = a^{\mu b^{\nu\}} + a^{\nu b^{\mu\}}$ , and  $M$  is the hadron mass.

For obtaining possible TMDs and PDFs, the correlation function is decomposed by considering the Hermiticity and parity invariance as [39]

Quark	U ( $\gamma^+$ )		L ( $\gamma^+\gamma_5$ )		T ( $i\sigma^+\gamma_5/\sigma^+$ )	
	T-even	T-odd	T-even	T-odd	T-even	T-odd
U	$f_1$					$[h_1^+]$
L			$g_{1L}$			$[h_{1L}^+]$
T		$f_{1T}^+$	$g_{1T}$		$[h_{1T}, h_{1T}^+]$	
LL	$f_{1LL}$					$[h_{1LL}^+]$
LT	$f_{1LT}$		$g_{1LT}$		$[h_{1LT}, h_{1LT}^+]$	
TT	$f_{1TT}$		$g_{1TT}$		$[h_{1TT}, h_{1TT}^+]$	

Table 2 Twist-2 TMDs.

Quark	$\gamma^+, 1, i\gamma_5$		$\gamma^+\gamma_5$		$\sigma^+, \sigma^+$	
	T-even	T-odd	T-even	T-odd	T-even	T-odd
U	$f_1^+$	$[e]$			$g^+$	$[h]$
L		$f_{1L}^+$	$g_{1L}^+$			$[h_{1L}]$
T		$f_{1T}^+, f_{1T}^+$	$g_{1T}, g_{1T}^+$			$[h_{1T}, h_{1T}^+]$
LL	$f_{1LL}^+$	$[e_{1L}]$			$g_{1LL}^+$	$[h_{1LL}]$
LT	$f_{1LT}^+, f_{1LT}^+$	$[e_{1L}, e_{1L}^+]$	$g_{1LT}, g_{1LT}^+$			$[h_{1LT}, h_{1LT}^+]$
TT	$f_{1TT}^+, f_{1TT}^+$	$[e_{1T}, e_{1T}^+]$	$g_{1TT}, g_{1TT}^+$			$[h_{1TT}, h_{1TT}^+]$

Table 3 Twist-3 TMDs.

Quark	$\gamma^-$		$\gamma^-\gamma_5$		$\sigma^-, \sigma^-$	
	T-even	T-odd	T-even	T-odd	T-even	T-odd
U	$f_3$					$[h_3^-]$
L			$g_{3L}$			$[h_{3L}^-]$
T		$f_{3T}^-$	$g_{3T}$		$[h_{3T}, h_{3T}^-]$	
LL	$f_{3LL}$					$[h_{3LL}^-]$
LT	$f_{3LT}$		$g_{3LT}$		$[h_{3LT}, h_{3LT}^-]$	
TT	$f_{3TT}$		$g_{3TT}$		$[h_{3TT}, h_{3TT}^-]$	

Table 4 Twist-4 TMDs.

Quark	U ( $\gamma^+$ )		L ( $\gamma^+\gamma_5$ )		T ( $i\sigma^+\gamma_5/\sigma^+$ )	
	T-even	T-odd	T-even	T-odd	T-even	T-odd
U	$f_1$					
L			$g_{1L}(g)$			
T					$[h_1]$	
LL	$f_{1LL}(b)$					
LT					$*1 [h_{1LT}]$	
TT						

Table 5 Twist-2 PDFs.

Quark	$\gamma^+, 1, i\gamma_5$		$\gamma^+\gamma_5$		$\sigma^+, \sigma^+$	
	T-even	T-odd	T-even	T-odd	T-even	T-odd
U	$[e]$					
L					$[h_{1L}]$	
T			$g_T$			
LL	$[e_{1L}]$				$*3 [h_{1LL}]$	
LT	$f_{1LT}$			$*2 g_{1LT}$		
TT						

Table 6 Twist-3 PDFs.

Quark	$\gamma^-$		$\gamma^-\gamma_5$		$\sigma^-, \sigma^-$	
	T-even	T-odd	T-even	T-odd	T-even	T-odd
U	$f_3$					
L			$g_{3L}$			
T					$[h_{3T}]$	
LL	$f_{3LL}$					
LT					$*4 [h_{3LT}]$	
TT						

Table 7 Twist-4 PDFs.

$$\Phi(k, P, T | n) = \frac{A_{13}}{M} T_{kk} + \dots + \frac{A_{20}}{M^2} \varepsilon^{\mu\nu Pk} \gamma_\mu \gamma_5 T_{\nu k} + \frac{B_{21} M}{P \cdot n} T_{kn} + \dots + \frac{B_{52} M}{P \cdot n} \sigma_{\mu k} T^{\mu n}, \quad (28)$$

where the contraction is defined as  $X_{\mu k} \equiv X_{\mu\nu} k^\nu$ , by extending the twist-2 expression in Ref. [34] with the additional  $n$ -dependent terms for studying twist-3 and twist-4 TMDs and PDFs. Then, the TMDs and collinear correlation functions are given by integrating it over the quark momenta as

$$\Phi^{[c]}(x, k_T, P, T) = \int dk^+ dk^- \Phi^{[c]}(k, P, T | n) \delta(k^+ - xP^+),$$

$$\Phi(x, P, T) = \int d^2 k_T \Phi^{[c]}(x, k_T, P, T). \quad (29)$$

Possible TMDs and PDFs are obtained by the traces of these correlation functions with  $\gamma$  matrices ( $\Gamma$ ) as  $\Phi^{[\Gamma]} \equiv \frac{1}{2} \text{Tr}[\Phi \Gamma]$ . The twist-2 TMDs and PDFs are defined by the traces  $\Phi^{[\gamma^+]}$ ,  $\Phi^{[\gamma^+\gamma_5]}$ , and  $\Phi^{[i\sigma^{i+}\gamma_5]}$  (or  $\Phi^{[\sigma^{i+}]}$ ), the twist-3 functions are by  $\Phi^{[\gamma^i]}$ ,  $\Phi^{[1]}$ ,  $\Phi^{[i\gamma_5]}$ ,  $\Phi^{[\gamma^i\gamma_5]}$ ,  $\Phi^{[\sigma^{ij}]}$ , and  $\Phi^{[\sigma^{-+}]}$ , where  $i$  and  $j$  are transverse indices ( $i, j = 1$  or  $2$ ), and the twist-4 functions are by  $\Phi^{[\gamma^-]}$ ,  $\Phi^{[\gamma^-\gamma_5]}$ , and  $\Phi^{[\sigma^{i-}]}$  as shown in Tables 2–7. As an example for the twist-3 TMDs, we have the relation

$$\Phi^{[\gamma^i]}(x, k_T, T) = \frac{M}{P^+} \left[ f_{LL}^\perp(x, k_T^2) S_{LL} \frac{k_T^i}{M} + f_{LT}^\perp(x, k_T^2) S_{LT}^i - f_{LT}^\perp(x, k_T^2) \frac{k_T^i S_{LT} \cdot k_T}{M^2} - f_{TT}^\perp(x, k_T^2) \frac{S_{TT}^{ij} k_{Tj}}{M} + f_{TT}^\perp(x, k_T^2) \frac{k_T \cdot S_{TT} \cdot k_T}{M^2} \frac{k_T^i}{M} \right]. \quad (30)$$

In Table 3, the TMDs without  $'$  are shown by defining  $F(x, k_T^2) \equiv F'(x, k_T^2) - (k_T^2/(2M^2)) F^\perp(x, k_T^2)$  where  $k_T^2 = -\mathbf{k}_T^2$ . From these studies, we found that there are

40 TMDs in total, and they are 10, 20, and 10 tensor-polarized TMDs at twists 2, 3, and 4, respectively, as

$$\text{Twist-2 TMD: } f_{1LL}, f_{1LT}, f_{1TT}, g_{1LT}, g_{1TT}, h_{1LL}^\perp, h_{1LT}^\perp, h_{1LT}^\perp, h_{1TT}^\perp, h_{1TT}^\perp,$$

$$\text{Twist-3 TMD: } f_{LL}^\perp, e_{LL}, f_{LT}^\perp, f_{LT}^\perp, e_{1T}, e_{1T}^\perp, f_{TT}, f_{TT}^\perp, e_{TT}, e_{TT}^\perp, g_{LL}^\perp, g_{LT}^\perp, g_{LT}^\perp, g_{TT}, g_{TT}^\perp, h_{1L}, h_{1LT}, h_{1LT}^\perp, h_{TT}, h_{TT}^\perp,$$

$$\text{Twist-4 TMD: } f_{3LL}, f_{3LT}, f_{3TT}, g_{3LT}, g_{3TT}, h_{3LL}^\perp, h_{3LT}^\perp, h_{3LT}^\perp, h_{3TT}, h_{3TT}^\perp. \quad (31)$$

In Tables 2, 3, and 4, the TMDs are classified by chiral even/odd and time-reversal even/odd. Chiral-odd distributions are shown with the square brackets  $[ ]$ , and the distributions without the bracket are chiral-even ones. The polarizations U, L, and T indicate unpolarized, longitudinally polarized, and transversely polarized, respectively, and the tensor polarizations are shown by LL, LT, and TT. The asterisks \*1, \*2, \*3, \*4 mean that the PDFs  $h_{1LT}(x)$ ,  $g_{LT}(x)$ ,  $h_{LL}(x)$ ,  $h_{3LT}(x)$  vanish because of the time-reversal invariance; however, the corresponding fragmentation functions  $H_{1LT}(z)$ ,  $G_{LT}(z)$ ,  $H_{LL}(z)$ ,  $H_{3LT}(z)$  should exist as collinear fragmentation functions [39, 40], and finite transverse momentum moments could exist even for the T-odd TMDs. The time-reversal invariance should be satisfied for the collinear PDFs, so that there are sum rules for the T-odd TMDs by the integral over the transverse momentum  $\vec{k}_T$  as

$$\int d^2 k_T h_{1LT}(x, k_T^2) = \int d^2 k_T g_{LT}(x, k_T^2) = \int d^2 k_T h_{LL}(x, k_T^2) = \int d^2 k_T h_{3LT}(x, k_T^2) = 0. \quad (32)$$



The possible PDFs were obtained by integrating the TMDs over  $\mathbf{k}_T$  up to twist 4 as

$$\begin{aligned} \text{Twist-2 PDF: } & f_{1LL}, \\ \text{Twist-3: } & e_{LL}, f_{LT}, \\ \text{Twist-4: } & f_{3LL}. \end{aligned} \quad (33)$$

The distribution  $f_{1LL}$  corresponds to the tensor-polarized distribution  $\delta_{Tq}$  in Sec. 2 by the relation  $f_{1LL} = -(2/3)\delta_{Tq}$ . There are a twist-2 sum rule and useful relations among these PDFs and multiparton distribution functions [41, 42] as discussed in Sec. 3.2. In this way, we are ready to investigate the structure functions of spin-1 hadrons up to twist 4 in the similar way with those of the spin-1/2 nucleon.

### 3.2 Relations of twist 2 and from equation of motion

Because the higher-twist PDFs were obtained for the tensor-polarized spin-1 hadron as explained in Sec. 3.1, it is interesting to investigate whether there are useful relations among them to find their magnitudes and functional forms. In the spin-1/2 nucleon, there are a twist-2 relation called the Wandzura-Wilczek (WW) relation and the Burkhardt-Cottingham (BC) sum rule. Such relations were investigated for the twist-2 and twist-3 tensor-polarized PDFs  $f_{1LL}$  and  $f_{LT}$  [41] of spin-1 hadrons. We obtained a similar equation to the WW relation by using the operator product expansion and defining multiparton distribution functions for twist-3 terms as

$$f_{LT}(x) = \frac{3}{2} \int_x^{\epsilon(x)} \frac{dy}{y} f_{1LL}(y) + \int_x^{\epsilon(x)} \frac{dy}{y} f_{LT}^{(HT)}(y), \quad (34)$$

where  $\epsilon(x)$  is  $\epsilon(x) = 1$  ( $-1$ ) at  $x > 0$  ( $x < 0$ ), and the last term is the twist-3 term (HT: higher twist) given by the multiparton distribution functions. The + PDFs  $f^+(x)$  are defined by  $f^+(x) = f(x) + \bar{f}(x)$  in the range  $0 \leq x \leq 1$ . Then, the  $f_{1LL}^+$  is related to  $b_1$  by  $b_1^{q+\bar{q}} = -(3/2)f_{1LL}^+$ . If the higher-twist term is neglected, Eq. (34) became

$$f_{LT}^+(x) = \frac{3}{2} \int_x^1 \frac{dy}{y} f_{1LL}^+(y), \quad (35)$$

which indicates the twist-2 part of  $f_{LT}$  is expressed by an integral of the twist-2 distribution  $f_{1LL}$  (or  $b_1$ ). This equation was written in the similar form with the WW relation by defining  $f_{2LL}$  as  $f_{2LL} = \frac{2}{3}f_{LT} - f_{1LL}$ :

$$f_{2LT}^+(x) = -f_{1LL}^+(x) + \int_x^1 \frac{dy}{y} f_{1LL}^+(y).$$

By integrating this equation over  $x$ , the BC-like sum rule was obtained

$$\int_0^1 dx f_{2LT}^+(x) = 0.$$

If the  $b_1$  sum rule of Eq. (10) is used for  $f_{1LL}$  ( $b_1$ ), namely  $\int dx f_{1LL}^+(x) = 0$  ( $\int dx b_1^{q+\bar{q}}(x) = 0$ ), by assuming vanishing tensor-polarized antiquark distributions, a sum rule

$$\int_0^1 dx f_{LT}^+(x) = 0, \quad (36)$$

is satisfied for  $f_{LT}$  itself. In these studies, we found the existence of the tensor-polarized multiparton distribution functions  $F_{LT}(x, y)$ ,  $G_{LT}(x, y)$ ,  $H_{LL}^\perp(x, y)$ , and  $H_{TT}(x, y)$ .

Other useful relations were derived by using the equation of motion for quarks [42]. The transverse momentum moments of the TMDs are defined by  $f^{(1)}(x) = \int d^2k_T (\vec{k}_T^2 / (2M^2)) f(x, k_T^2)$ . The first relation is for the twist-3 PDF  $f_{LT}$ , the transverse-momentum moment PDF  $f_{1LT}^{(1)}$ , and the multiparton distribution functions  $F_{G,LT}$  and  $G_{G,LT}$ :

$$\begin{aligned} x f_{LT}(x) - f_{1LT}^{(1)}(x) \\ - \mathcal{P} \int_{-1}^1 dy \frac{F_{G,LT}(x, y) + G_{G,LT}(x, y)}{x - y} = 0, \end{aligned} \quad (37)$$

where  $\mathcal{P}$  is the principle integral. Next, the second relation is for the twist-3 PDF  $e_{LL}$ , the twist-2 PDF  $f_{1LL}$ , and the multiparton distribution function  $H_{G,LL}^\perp$ :

$$x e_{LL}(x) - 2\mathcal{P} \int_{-1}^1 dy \frac{H_{G,LL}^\perp(x, y)}{x - y} - \frac{m}{M} f_{1LL}(x) = 0, \quad (38)$$

where  $m$  is the quark mass. The third relation is the Lorentz-invariance relation:

$$\begin{aligned} \frac{df_{1LT}^{(1)}(x)}{dx} - f_{LT}(x) + \frac{3}{2} f_{1LL}(x) \\ - 2\mathcal{P} \int_{-1}^1 dy \frac{F_{G,LT}(x, y)}{(x - y)^2} = 0. \end{aligned} \quad (39)$$

The relations among the multiparton distribution functions  $F_{D/G,LT}(x, y)$ ,  $G_{D/G,LT}(x, y)$ ,  $H_{D/G,LL}^\perp(x, y)$ , and  $H_{D/G,TT}(x, y)$  were also obtained.

## 4 Fragmentation functions

The collinear fragmentation functions (FFs) for spin-1 hadrons were investigated up to twist 4 in Ref. [40]. However, consistent derivations on the TMD FFs of the spin-1 hadrons were restricted to the twist-2 until recently, and the TMDs FFs were obtained up to twist 4 in Ref. [39]. The collinear FFs and TMD FFs are obtained from the PDFs and TMDs, respectively, simply by changing the variables and function names as [34, 39]

$$\begin{aligned} \text{Kinematical variables: } & x, k_T, S, T, M, n, \gamma^+, \sigma^{i+} \\ & \Rightarrow z, k_T, S_h, T_h, M_h, \bar{n}, \gamma^-, \sigma^{i-}, \end{aligned}$$

Quark	U ( $\gamma^*$ )		L ( $\gamma^* \gamma_5$ )		T ( $i\sigma^* \gamma_5 / \sigma^*$ )	
	T-even	T-odd	T-even	T-odd	T-even	T-odd
U	$D_1$					$ H_1^* $
L			$G_{1L}$			$ H_{1L}^* $
T		$D_{1T}^*$	$G_{1T}$			$ H_{1T} ,  H_{1T}^* $
LL	$D_{1LL}$					$ H_{1LL}^* $
LT	$D_{1LT}$		$G_{1LT}$			$ H_{1LT} ,  H_{1LT}^* $
TT	$D_{1TT}$		$G_{1TT}$			$ H_{1TT} ,  H_{1TT}^* $

Table 8 Twist-2 TMD FFs.

Quark	$\gamma^*, 1, i\gamma_5$		$\gamma^* \gamma_5$		$\sigma^*, \sigma^*$	
	T-even	T-odd	T-even	T-odd	T-even	T-odd
U	$D^*$	$ E $			$G^*$	$ H $
L		$D_{1L}^*$	$G_{1L}^*$			$ H_{1L} $
T		$D_{1T}, D_{1T}^*$	$G_{1T}, G_{1T}^*$			$ H_{1T} ,  H_{1T}^* $
LL	$D_{1LL}^*$	$ E_{1L} $			$G_{1LL}^*$	$ H_{1LL} $
LT	$D_{1LT}, D_{1LT}^*$	$ E_{1L}, E_{1L}^* $			$G_{1LT}, G_{1LT}^*$	$ H_{1LT} ,  H_{1LT}^* $
TT	$D_{1TT}, D_{1TT}^*$	$ E_{1T}, E_{1T}^* $			$G_{1TT}, G_{1TT}^*$	$ H_{1TT} ,  H_{1TT}^* $

Table 9 Twist-3 TMD FFs.

Quark	$\gamma^-$		$\gamma^- \gamma_5$		$\sigma^-$	
	T-even	T-odd	T-even	T-odd	T-even	T-odd
U	$D_3$					$ H_3^* $
L			$G_{3L}$			$ H_{3L}^* $
T		$D_{3T}^*$	$G_{3T}$			$ H_{3T} ,  H_{3T}^* $
LL	$D_{3LL}$	$ E_{3L} $				$ H_{3LL}^* $
LT	$D_{3LT}$		$G_{3LT}$			$ H_{3LT} ,  H_{3LT}^* $
TT	$D_{3TT}$		$G_{3TT}$			$ H_{3TT} ,  H_{3TT}^* $

Table 10 Twist-4 TMD FFs.

Quark	U ( $\gamma^*$ )		L ( $\gamma^* \gamma_5$ )		T ( $i\sigma^* \gamma_5 / \sigma^*$ )	
	T-even	T-odd	T-even	T-odd	T-even	T-odd
U	$D_1$					
L			$G_{1L}$			
T					$ H_1 $	
LL	$D_{1LL}$					
LT					$ H_{1LT} $	
TT						

Table 11 Twist-2 FFs.

Quark	$\gamma^*, 1, i\gamma_5$		$\gamma^* \gamma_5$		$\sigma^*, \sigma^*$	
	T-even	T-odd	T-even	T-odd	T-even	T-odd
U	$ E $					
L					$ H_{1L} $	
T			$G_{1T}$			
LL	$ E_{1L} $				$ H_{1LL} $	
LT	$D_{1LT}$		$G_{1LT}$			
TT						

Table 12 Twist-3 FFs.

Quark	$\gamma^-$		$\gamma^- \gamma_5$		$\sigma^-$	
	T-even	T-odd	T-even	T-odd	T-even	T-odd
U	$D_3$					
L			$G_{3L}$			
T					$ H_{3T} $	
LL	$D_{3LL}$					
LT					$ H_{3LT} $	
TT						

Table 13 Twist-4 FFs.

Distribution functions:  $f, g, h, e$   
 $\Rightarrow$  Fragmentation functions:  $D, G, H, E$ . (40)

For spin-1 hadrons, the twist-2, 3, and 4 TMD FFs are listed in Tables 8, 9, and 10, and the twist-2, 3, and 4 collinear FFs are listed in Tables 11, 12, and 13. As mentioned in Sec. 3 for the asterisks of Tables 5, 6, and 7, the corresponding T-odd collinear fragmentation functions exist, although the T-odd PDFs do not exist, because the time-reversal invariance does not have to be imposed in the FFs. These collinear and TMD FFs could be investigated experimentally by future experiments.

In the similar way to the PDFs, there are relations among the FFs and the multiparton distributions [43]. First, the equation of motion for quarks leads to the relations

$$E_{LL}(z) + iH_{LL}(z) - \frac{m_q}{M} z D_{1LL}(z) = 2z \left[ -iH_{1LL}^{\perp(1)}(z) + \mathcal{P} \int_z^\infty \frac{dz_1}{(z_1)^2} \frac{H_{G,LL}^\perp(z, z_1)}{\frac{1}{z} - \frac{1}{z_1}} \right], \quad (41)$$

$$D_{LT}(z) + iG_{LT}(z) + \frac{im_q}{M} z H_{1LT}(z) = -z \left[ iG_{1LT}^{(1)}(z) - \int_z^\infty \frac{dz_1}{(z_1)^2} \frac{G_{G,LT}(z, z_1)}{\frac{1}{z} - \frac{1}{z_1}} \right] - z \left[ D_{1LT}^{(1)}(z) + \int_z^\infty \frac{dz_1}{(z_1)^2} \frac{D_{G,LT}(z, z_1)}{\frac{1}{z} - \frac{1}{z_1}} \right], \quad (42)$$

$$iH_{1TT}^{(1)}(z) + \int_z^\infty \frac{dz_1}{(z_1)^2} \frac{H_{G,TT}(z, z_1)}{\frac{1}{z} - \frac{1}{z_1}} = 0. \quad (43)$$

There are also Lorentz-invariance relations

$$\frac{3}{2} D_{1LL}(z) - D_{LT}(z) - z \left( 1 - z \frac{d}{dz} \right) D_{1LT}^{(1)}(z) = -2 \int_z^\infty \frac{dz_1}{(z_1)^2} \frac{\text{Re}[D_{G,LT}(z, z_1)]}{\left( \frac{1}{z} - \frac{1}{z_1} \right)^2}, \quad (44)$$

$$H_{LL}(z) + 2H_{1LT}(z) + z \left( 1 - z \frac{d}{dz} \right) H_{1LL}^{\perp(1)}(z) = -2 \int_z^\infty \frac{dz_1}{(z_1)^2} \frac{\text{Im}[H_{G,LL}^\perp(z, z_1)]}{\left( \frac{1}{z} - \frac{1}{z_1} \right)^2}, \quad (45)$$

$$G_{LT}(z) + z \left( 1 - z \frac{d}{dz} \right) G_{1LT}^{(1)}(z) = -2 \int_z^\infty \frac{dz_1}{(z_1)^2} \frac{\text{Im}[G_{G,LT}(z, z_1)]}{\left( \frac{1}{z} - \frac{1}{z_1} \right)^2}. \quad (46)$$

These relations are useful in studying the twist-3 FFs in future.

Note added: In this paper, we did not have space to discuss the generalized parton distributions for spin-1 hadrons. We list references [44, 45] for understanding the current status. There were lightcone-model studies on the spin-1  $\rho$ -meson GPDs [46, 47] and TMDs [48, 49].

## 5 Summary

Polarized structure functions have not been investigated for the spin-1 hadrons except for the HERMES measurement on  $b_1$ ; however, the situation will change in a few years due to the JLab project on the tensor-polarized spin-1 deuteron. Furthermore, they could be

investigated at Fermilab by the proton-deuteron Drell-Yan processes, and the polarized deuteron beams will be available at NICA and EICs. Theoretical tools are ready up to twist 4 for the collinear PDFs, the TMDs, the collinear fragmentation functions, and TMD fragmentation functions. For example, the tensor-polarized structure function  $b_1$  and the gluon transversity associated with the deuteron's linear polarization could indicate a new hadron physics beyond the basic deuteron description in terms of a bound system of a proton and a neutron. From the future experimental measurements, there is a possibility that a new field of hadron physics could be created.

## 6 Acknowledgements

SK was partially supported by Japan Society for the Promotion of Science (JSPS) Grants-in-Aid for Scientific Research (KAKENHI) Grant Number 24K07026.

## References

1. R. Abdul Khalek, *et al.*, Nucl. Phys. A **1026**, 122447 (2022)
2. D. Anderle, *et al.*, Front. Phys. **16**, 64701 (2021)
3. A. Airapetian, *et al.* (HERMES Collaboration), Phys. Rev. Lett. **95**, 242001 (2005)
4. K. Allada, *et al.*, Proposal to Jefferson Lab PAC-51, PR12-13-011, [https://www.jlab.org/exp\\_prog/proposals/13/PR12-13-011.pdf](https://www.jlab.org/exp_prog/proposals/13/PR12-13-011.pdf) (2023)
5. J. Maxwell, *et al.*, arXiv: 1803.11206 (2018)
6. M. Brooks, *et al.*, [https://twist.phys.virginia.edu/work/E1039proposal\\_final.pdf](https://twist.phys.virginia.edu/work/E1039proposal_final.pdf); SinQest Collaboration, <https://spinquest.fnal.gov/> (2017)
7. D. Keller, arXiv: 2205.01249 (2022)
8. A. Arbuzov, *et al.*, Prog. Part. Nucl. Phys. **119**, 103858 (2021)
9. L. Frankfurt, M. Strikman, Nucl. Phys. A **405**, 557 (1983)
10. P. Hoodbhoy, R. Jaffe, A. Manohar, Nucl. Phys. B **312**, 571 (1989)
11. W. Cosyn, Y.B. Dong, S. Kumano, M. Sargsian, Phys. Rev. D **95**, 074036 (2017)
12. R. Jaffe, A. Manohar, Phys. Lett. B **223**, 218 (1989)
13. T.Y. Kimura, S. Kumano, Phys. Rev. D **78**, 117505 (2008)
14. S. Kumano, J. Phys. Conf. Ser. **543**, 012001 (2014)
15. R. Jaffe, A. Manohar, Nucl. Phys. B **321**, 343 (1989)
16. F.E. Close, S. Kumano, Phys. Rev. D **42**, 2377 (1990)
17. R.P. Feynman, p.91, Photon-Hadron Interactions, W. A. Benjamin, Inc. (1972)
18. S. Kumano, Phys. Rep. **303**, 183 (1998)
19. G. Garvey, J.C. Peng, Prog. Part. Nucl. Phys. **47**, 203 (2001)
20. J.C. Peng, J.W. Qiu, Prog. Part. Nucl. Phys. **76**, 43 (2014)
21. A.V. Efremov, O.V. Teryaev, Sov. J. Nucl. Phys. **36**, 557 (1982)
22. G.A. Miller, Phys. Rev. C **89**, 045203 (2014)
23. S. Kumano, Phys. Rev. D **82**, 017501 (2010)
24. S. Kumano, Q.T. Song, Phys. Rev. D **94**, 054022 (2016)
25. S. Hino, S. Kumano, Phys. Rev. D **59**, 094026 (1999); **60**, 054018 (1999)
26. S. Kumano, M. Miyama, Phys. Lett. B **479**, 149 (2000)
27. S. Kumano, Q.T. Song, Phys. Rev. D **101**, 054011 (2020); **101**, 094013 (2020)
28. X. Artru, M. Mekhfi, Z. Phys. C **45**, 669 (1990)
29. P.J. Mulders, J. Rodrigues, Phys. Rev. D **63**, 094021 (2001)
30. M. Nzar, P. Hoodbhoy, Phys. Rev. D **45**, 2264 (1992)
31. W. Vogelsang, Acta Phys. Pol. B **29**, 1189 (1998)
32. E. Sather, C. Schmidt, Phys. Rev. D **42**, 1424 (1990)
33. W. Detmold, P.E. Shanahan, Phys. Rev. D **94**, 014507 (2016); Erratum, **95**, 079902 (2017)
34. A. Bacchetta, P.J. Mulders, Phys. Rev. D **62**, 114004 (2000)
35. D. Boer, *et al.*, J. High Energy Phys. **2016**, 13 (2016)
36. S. Meißner, A. Metz, K. Goeke, Phys. Rev. D **76**, 034002 (2007)
37. G. Sterman, *et al.*, Rev. Mod. Phys. **67**, 157 (1995)
38. J.P. Ma, C. Wang, G.P. Zhang, arXiv: 1306.6693 (2013)
39. S. Kumano, Q.T. Song, Phys. Rev. D **103**, 014025 (2021)
40. X. Ji, Phys. Rev. D **49**, 114 (1994)
41. S. Kumano, Q.T. Song, J. High Energy Phys. **2021**, 141 (2021)
42. S. Kumano, Q.T. Song, Phys. Lett. B **826**, 136908 (2022)
43. Q.T. Song, Phys. Rev. D **108**, 094041 (2023)
44. E.R. Berger, F. Cano, M. Diehl, B. Pire, Phys. Rev. Lett. **87**, 142302 (2001)
45. W. Cosyn, B. Pire, Phys. Rev. D **98**, 074020 (2018)
46. B.D. Sun, Y.B. Dong, Phys. Rev. D **96**, 036019 (2017); **99**, 016023 (2019); **101**, 096008 (2020)
47. N. Kumar, Phys. Rev. D **99**, 014039 (2019)
48. C. Shi, *et al.*, Phys. Rev. D **106**, 014026 (2022)
49. S. Kaur, *et al.*, Phys. Lett. B **851**, 138563 (2024)